

Spatial-Network Treatment Effects: A Continuous Functional Approach

Tatsuru Kikuchi*

*Center for Advanced Research in Finance, The University of Tokyo,
7-3-1 Hongo, Bunkyo-ku, Tokyo 113-0033 Japan*

(December 18, 2025)

Abstract

This paper develops a continuous functional framework for treatment effects that propagate through geographic space and economic networks. We derive a master equation governing propagation from three economic foundations—heterogeneous agent aggregation, market equilibrium, and cost minimization—establishing that the framework rests on fundamental principles rather than ad hoc specifications. A key result shows that the spatial-network interaction coefficient equals the mutual information between geographic and market coordinates. The Feynman-Kac representation decomposes effects into inherited and accumulated components along stochastic paths representing economic linkages. The framework nests the no-spillover case as a testable restriction. Monte Carlo simulations demonstrate that conventional estimators—two-way fixed effects, difference-in-differences, and generalized propensity score—exhibit 25–38% bias and severe undercoverage when spillovers exist, while our estimator

*e-mail: tatsuru.kikuchi@e.u-tokyo.ac.jp

maintains correct inference regardless of whether spillovers are present. Applying the framework to U.S. minimum wage policy, we reject the no-spillover null and find total effects at state borders four times larger than direct effects—conventional methods capture only one-quarter of policy impact. Structural estimates reveal spatial diffusion consistent with commuting-distance labor mobility, network diffusion consistent with quarterly supply chain adjustment, and significant spatial-network interaction reflecting geographic clustering of industries.

JEL Classification: C21, C23, J31, J38, R12

Keywords: treatment effects, spatial econometrics, network spillovers, continuous treatment

1 Introduction

Treatment effects in interconnected economies propagate beyond directly treated units through two fundamental channels: geographic proximity and economic networks. These spillovers violate the stable unit treatment value assumption (SUTVA) underlying standard econometric methods, causing systematic bias in treatment effect estimates. Moreover, spatial and network spillovers interact synergistically when geographic proximity correlates with economic connections, creating amplification effects that additive specifications miss entirely. Standard methods—two-way fixed effects, difference-in-differences, generalized propensity scores—cannot accommodate these features, leading to substantial understatement of policy impacts when spillovers are empirically relevant.

For example, when California raises its minimum wage, wages rise not only in California but also in neighboring Nevada counties through labor market competition, as workers commute across borders and firms compete for employees in integrated labor markets. Simultaneously, wages rise in upstream industries throughout the western United States through supply chain cost transmission, as California firms pass higher labor costs to suppliers regardless of their geographic location. Most importantly, wage effects are largest in Nevada border counties with dense supply chain connections to California industries—regions where both spatial proximity and network linkages expose workers to the policy shock. This spatial-network interaction amplifies total effects beyond what either channel alone would predict, yet conventional methods that include spatial and network terms separately but omit their interaction miss this amplification entirely. Similar propagation patterns arise in other policy contexts: financial regulations transmit through both geographic banking markets and interbank lending networks; trade policies propagate through both border regions and global supply chains; technology adoption spreads through both local demonstration effects and industry knowledge networks.

This paper develops a unified framework for treatment effects that propagate

through both geographic space and economic networks in continuous time. The continuous functional representation—treating treatment intensity as a smooth function $\tau(\mathbf{x}, t, \alpha)$ over spatial coordinates \mathbf{x} , time t , and market position α —resolves fundamental limitations of discrete methods that force arbitrary boundaries between treated and control units. The framework captures spatial-network interaction through a theoretically grounded coefficient that equals the mutual information between geographic and market coordinates, providing a parameter-free measure of channel complementarity. The dynamic structure characterizes how treatment effects evolve as markets adjust toward new equilibria, with diffusion coefficients measuring the speed of spatial and network propagation and decay parameters measuring market adjustment rates.

1.1 Contributions

The paper makes three main contributions spanning theory, methodology, and empirics.

Theoretical Contribution The theoretical contribution derives a master equation governing treatment propagation from three independent economic foundations: heterogeneous agent aggregation following the tradition of Aiyagari (1994) and Huggett (1993), market equilibrium conditions connecting volatility to dynamic adjustment, and cost minimization principles underlying market equilibrium. The convergence of these derivations—each starting from different economic primitives but arriving at the same equation—establishes that the framework rests on fundamental economic principles rather than ad hoc specifications. The master equation

$$\frac{\partial \tau}{\partial t} = \nu_s \nabla^2 \tau + \nu_n \frac{\partial^2 \tau}{\partial \alpha^2} - \kappa \tau + \lambda D_s D_n + S \quad (1)$$

unifies spatial diffusion (coefficient ν_s reflecting labor mobility), network propagation (ν_n reflecting supply chain fluidity), market adjustment (κ reflecting equilibration speed), spatial-network interaction (λ), and policy intervention (S) within a single analytical structure. Each parameter has a structural interpretation grounded in the underlying economic primitives.

A key theoretical result establishes that the spatial-network interaction coefficient λ equals the mutual information between geographic and market coordinates. This information-theoretic characterization provides a parameter-free measure of channel complementarity grounded in the entropy concepts of Cover and Thomas (2006) rather than functional form assumptions. The Feynman-Kac representation connects the partial differential equation framework to economic intuition: treatment effects at any location reflect accumulated policy exposure along stochastic paths representing economic linkages—workers migrating, firms adjusting supply chains, prices equilibrating across connected markets.

Methodological Contribution The methodological contribution demonstrates that the framework nests the no-spillover case as a testable restriction. When $\nu_s = \nu_n = 0$, the master equation reduces to independent dynamics at each location, recovering standard continuous treatment estimation following Hirano and Imbens (2004) and Kennedy et al. (2017). This nested structure creates a one-sided risk profile: when spillovers are absent, the framework correctly detects this and produces estimates equivalent to conventional methods; when spillovers are present, the framework captures them while conventional methods fail.

We develop a comprehensive identification strategy combining three complementary approaches: spatial regression discontinuity exploiting sharp policy boundaries at state borders, network instrumental variables using predetermined supply chain connections, and entropy-based moment conditions leveraging theoretical predictions. Monte Carlo simulations with both binary treatment timing and continuous treatment

intensity demonstrate that two-way fixed effects, heterogeneity-robust difference-in-differences, and generalized propensity score estimators exhibit 25–38% bias and 52–68% confidence interval coverage when spillovers of empirically relevant magnitude exist, while our estimator maintains correct inference across all configurations.

Empirical Contribution The empirical contribution applies the framework to U.S. minimum wage policy, testing the no-spillover null and estimating structural propagation parameters. We reject the no-spillover null at $p < 0.001$ and find that total effects at state borders are four times larger than direct effects alone—conventional methods capture only one-quarter of policy impact. Structural estimates reveal spatial diffusion consistent with commuting-distance labor mobility, network diffusion consistent with quarterly supply chain adjustment, and significant spatial-network interaction reflecting geographic clustering of industries.

1.2 Related Literature

This paper contributes to several literatures that have developed largely independently.

Spatial Econometrics and Spatial Inference The spatial econometrics literature, surveyed by Anselin (2010) and formalized by LeSage and Pace (2009), models spillovers through spatial weight matrices capturing geographic proximity. This approach assumes spillovers decay with distance according to prespecified functional forms and cannot accommodate network connections that operate independent of geography. Conley (1999) develops spatial HAC inference but does not address network dependence.

Recent work by Müller and Watson (2022) develops spatial correlation robust inference that remains valid under unknown forms of spatial dependence, providing confidence intervals with correct coverage regardless of the spatial correlation structure.

Their approach addresses the critical problem that standard spatial HAC estimators require correct specification of spatial correlation decay. Müller and Watson (2024) further establishes conditions under which spatial data exhibit unit root behavior, leading to spurious regression phenomena analogous to time series contexts. These papers highlight fundamental inferential challenges in spatial settings that motivate careful attention to dependence structures. Our framework complements this literature by deriving the spatial dependence structure from economic primitives—the master equation implies specific correlation patterns determined by the diffusion and decay parameters—enabling counterfactual analysis that purely statistical approaches cannot provide.

Network Econometrics The network econometrics literature, including Bramoullé et al. (2009) on peer effects identification and Jackson (2008) on network formation, addresses spillovers through social and economic connections. However, this literature typically treats network position as discrete (node membership) rather than continuous, ignoring geographic variation in network effects. Acemoglu et al. (2012) and Barrot and Sauvagnat (2016) document production network propagation but estimate reduced-form effects rather than structural propagation parameters. Our framework integrates network and spatial dimensions, models network position as continuous market coordinates, and recovers structural parameters governing propagation dynamics.

Treatment Effects Under Interference The treatment effects literature has developed sophisticated methods for heterogeneity and selection, including generalized propensity scores for continuous treatments (Hirano and Imbens, 2004), doubly robust estimation (Kennedy et al., 2017), and heterogeneity-robust difference-in-differences (Callaway and Sant’Anna, 2021; Sun and Abraham, 2021; Goodman-Bacon, 2021). These advances address important problems but maintain SUTVA, ruling out spillovers by assumption.

A growing literature relaxes SUTVA to allow interference, including Hudgens and Halloran (2008) on partial interference and Athey et al. (2018) on experimental design under interference. However, this literature typically assumes known interference structure rather than estimating propagation dynamics from data. Our framework estimates the interference structure—the diffusion coefficients (ν_s, ν_n) governing how treatment propagates—rather than assuming it known.

1.3 Outline

Section 2 develops the theoretical framework from microeconomic foundations, deriving the master equation from heterogeneous agent behavior, market equilibrium, and cost minimization, and establishing the Feynman-Kac representation and mutual information characterization. Section 3 establishes identification conditions, develops the no-spillover benchmark as a testable special case, presents comprehensive Monte Carlo evidence, and develops the GMM estimation framework with spatial-network HAC inference. Section 4 summarizes the empirical application to minimum wage spillovers. Section 5 concludes.

2 Theoretical Framework

This section derives the master equation governing treatment propagation from three independent economic foundations and establishes the key theoretical results: the Feynman-Kac representation and the mutual information characterization of spatial-network interaction.

2.1 Coordinate System and Treatment Representation

We represent economic units by coordinates (\mathbf{x}, α) where $\mathbf{x} \in \Omega \subseteq \mathbb{R}^d$ denotes spatial location and $\alpha \in \mathcal{I} \subseteq \mathbb{R}$ denotes market position. The treatment functional $\tau(\mathbf{x}, t, \alpha) :$

$\Omega \times [0, T] \times \mathcal{I} \rightarrow \mathbb{R}$ represents treatment intensity at each point in this coordinate space.

Definition 1 (Spatial and Network Coordinates). *The spatial coordinate \mathbf{x} represents geographic location—latitude, longitude, and potentially economic distance metrics reflecting transportation costs or commuting times.*

The market position coordinate α represents position in economic networks—production stage in supply chains, skill level in labor markets, or risk profile in financial networks.

The continuous representation avoids three limitations of discrete methods. First, it avoids arbitrary discretization of treatment intensity into binary indicators, preserving the dose-response relationship central to continuous treatment analysis. Second, it avoids arbitrary spatial boundaries between regions, allowing smooth geographic variation. Third, it avoids discrete network categories, enabling continuous market position that captures fine gradations in supply chain relationships or skill levels.

Definition 2 (Source Term). *The source term $S(\mathbf{x}, t, \alpha)$ represents the exogenous policy intervention entering the system. For minimum wage policy, S equals the dollar amount by which the new minimum wage exceeds the market-clearing wage at each location-time-industry cell.*

The distinction between source S and treatment functional τ is fundamental. The source is directly observable from policy variation; the treatment functional represents the equilibrium response incorporating both direct effects and all spillovers. The identification challenge is recovering τ (or its parameters) from observable variation in S and outcomes Y .

2.2 Derivation from Heterogeneous Agent Aggregation

The first derivation proceeds from aggregating heterogeneous agent behavior, following the tradition of Aiyagari (1994) and Huggett (1993) in macroeconomics.

Consider a continuum of heterogeneous agents indexed by type $\theta \in \Theta$ distributed over space and market positions. Each agent has idiosyncratic characteristics—productivity, preferences, constraints—captured by θ . Agent i of type θ at location \mathbf{x} with market position α experiences wage:

$$w_i(\mathbf{x}, t, \alpha, \theta) = w_0(\mathbf{x}, \alpha) + \tau(\mathbf{x}, t, \alpha) + \varepsilon_i(\theta) \quad (2)$$

where w_0 is the baseline wage, τ is the treatment effect to be determined, and $\varepsilon_i(\theta)$ captures idiosyncratic variation.

Agents optimize location and market position subject to mobility costs. The state of worker i evolves according to the stochastic differential equations:

$$dX_t^i = \mu_s(X_t^i, A_t^i, \theta_i) dt + \sigma_s(X_t^i, A_t^i, \theta_i) dB_t^s \quad (3)$$

$$dA_t^i = \mu_n(X_t^i, A_t^i, \theta_i) dt + \sigma_n(X_t^i, A_t^i, \theta_i) dB_t^n \quad (4)$$

where (B_t^s, B_t^n) are independent Brownian motions representing location and occupational uncertainty. The drift terms μ_s, μ_n capture directed mobility—workers moving toward higher wages or better opportunities. The diffusion terms σ_s, σ_n capture randomness in mobility outcomes—search frictions, information imperfections, unexpected opportunities.

The joint density $f(\mathbf{x}, t, \alpha)$ of agents over spatial and market coordinates evolves according to the Kolmogorov forward equation:

$$\frac{\partial f}{\partial t} = -\nabla \cdot (\boldsymbol{\mu}_s f) - \frac{\partial}{\partial \alpha} (\mu_n f) + \frac{1}{2} \nabla \cdot (\boldsymbol{\Sigma}_s \nabla f) + \frac{1}{2} \frac{\partial^2}{\partial \alpha^2} (\sigma_n^2 f) \quad (5)$$

This equation describes how the population distribution shifts as workers migrate and change occupations. The first two terms represent advection (directed flow); the last two terms represent diffusion (random spreading).

For the aggregate treatment effect, we average over agent types:

$$\tau(\mathbf{x}, t, \alpha) = \int_{\Theta} \tau(\mathbf{x}, t, \alpha, \theta) d\mu(\theta) \quad (6)$$

Proposition 1 (Aggregation Result). *Under the following regularity conditions:*

1. *Bounded heterogeneity: $\sup_{\theta} \|\sigma(\cdot, \theta)\| < \infty$*
2. *Ergodic agent dynamics: the process (X_t, A_t) has a unique stationary distribution for each θ*
3. *Smooth aggregation: the mapping $\theta \mapsto \tau(\cdot, \theta)$ is measurable*

the aggregate treatment functional satisfies:

$$\frac{\partial \tau}{\partial t} = \nu_s \nabla^2 \tau + \nu_n \frac{\partial^2 \tau}{\partial \alpha^2} - \kappa \tau + S(\mathbf{x}, t, \alpha) \quad (7)$$

where $\nu_s = \frac{1}{2} \mathbb{E}_{\theta}[\sigma_s^2(\theta)]$ is mean spatial diffusivity, $\nu_n = \frac{1}{2} \mathbb{E}_{\theta}[\sigma_n^2(\theta)]$ is mean network diffusivity, and κ reflects mean reversion from competitive pressure.

The aggregation result shows that heterogeneous agent behavior generates aggregate dynamics governed by a partial differential equation. The diffusion coefficients (ν_s, ν_n) emerge from averaging individual mobility variances across types; they measure how quickly treatment effects spread through the population as workers move and change occupations.

2.3 Derivation from Market Equilibrium

An independent derivation proceeds from market equilibrium conditions, connecting observed price volatility to underlying market structure.

In markets with search frictions, matching delays, or information asymmetries, prices fluctuate around equilibrium values. The observed volatility σ^2 of price processes relates to underlying market adjustment through the equilibrium volatility

relation:

$$\sigma^2 = 2D\kappa \tag{8}$$

where D is a diffusion coefficient measuring the amplitude of fluctuations and κ is the adjustment rate toward equilibrium.

This relation emerges from the stochastic process governing price dynamics:

$$dp = -\kappa(p - p^*) dt + \sigma dB \tag{9}$$

where p^* is the equilibrium price and κ governs the speed of mean reversion. At stationarity, the variance of the price distribution satisfies:

$$\text{Var}(p) = \frac{\sigma^2}{2\kappa} \tag{10}$$

Rearranging gives (8). The key insight is that market equilibrium connects two observable quantities—volatility σ^2 and adjustment speed κ —to the diffusion coefficient D governing spatial spreading.

Connecting observed wage dynamics to treatment propagation: spatial wage volatility σ_s^2 implies spatial diffusion $\nu_s = \sigma_s^2/(2\kappa)$; network wage volatility σ_n^2 implies network diffusion $\nu_n = \sigma_n^2/(2\kappa)$. Markets with high wage volatility (active reallocation, frequent job changes) exhibit rapid spatial diffusion; markets with low volatility exhibit slow diffusion.

This derivation provides an independent foundation for the diffusion coefficients in (7), grounding them in observable market dynamics rather than assumptions about individual behavior.

2.4 Derivation from Cost Minimization

A third derivation proceeds from cost minimization, following the variational principles underlying market equilibrium.

Definition 3 (Adjustment Cost Functional). *The total adjustment cost functional is:*

$$\mathcal{C}[\tau] = \int_0^T \int_{\Omega} \int_{\mathcal{I}} \left[\frac{1}{2} \left(\frac{\partial \tau}{\partial t} \right)^2 + \frac{\nu_s}{2} |\nabla \tau|^2 + \frac{\nu_n}{2} \left(\frac{\partial \tau}{\partial \alpha} \right)^2 + \frac{\kappa}{2} \tau^2 - S\tau \right] d\alpha d\mathbf{x} dt \quad (11)$$

The terms have economic interpretations:

- $\frac{1}{2}(\partial\tau/\partial t)^2$: Temporal adjustment costs. Rapidly changing wages are costly due to contracting frictions, menu costs, and coordination failures.
- $\frac{\nu_s}{2}|\nabla\tau|^2$: Spatial gradient costs. Maintaining wage differentials across space is costly due to arbitrage pressure from mobile workers.
- $\frac{\nu_n}{2}(\partial\tau/\partial\alpha)^2$: Network gradient costs. Maintaining wage differentials across market positions is costly due to substitution pressure in supply chains.
- $\frac{\kappa}{2}\tau^2$: Level costs. Deviating from baseline wages is costly due to competitive pressure.
- $-S\tau$: Policy benefits. The intervention S shifts the optimal wage structure.

Proposition 2 (Euler-Lagrange Equation). *The treatment functional τ^* minimizing $\mathcal{C}[\tau]$ satisfies:*

$$\frac{\partial \tau}{\partial t} = \nu_s \nabla^2 \tau + \nu_n \frac{\partial^2 \tau}{\partial \alpha^2} - \kappa \tau + S \quad (12)$$

Proof. The first variation of \mathcal{C} with respect to τ must vanish for all admissible variations η :

$$\delta \mathcal{C} = \int_0^T \int_{\Omega} \int_{\mathcal{I}} \left[\frac{\partial \tau}{\partial t} \frac{\partial \eta}{\partial t} + \nu_s \nabla \tau \cdot \nabla \eta + \nu_n \frac{\partial \tau}{\partial \alpha} \frac{\partial \eta}{\partial \alpha} + \kappa \tau \eta - S \eta \right] d\alpha d\mathbf{x} dt = 0 \quad (13)$$

Integrating by parts and assuming boundary terms vanish:

$$\int_0^T \int_{\Omega} \int_{\mathcal{I}} \left[-\frac{\partial^2 \tau}{\partial t^2} - \nu_s \nabla^2 \tau - \nu_n \frac{\partial^2 \tau}{\partial \alpha^2} + \kappa \tau - S \right] \eta d\alpha d\mathbf{x} dt = 0 \quad (14)$$

For this to hold for all η , the bracketed term must vanish. For quasi-static evolution where $\partial^2\tau/\partial t^2 \approx 0$ (gradual adjustment rather than oscillation), this yields the master equation. \square

The cost minimization derivation connects the master equation to optimization principles. The parameters (ν_s, ν_n, κ) have natural interpretations as relative costs of different types of adjustment: high ν_s means spatial arbitrage is rapid (low cost of spatial gradients); high κ means competitive pressure is strong (high cost of deviating from baseline).

2.5 The Complete Master Equation

The three derivations converge on the same structure but miss spatial-network interaction. When spatial and market coordinates are correlated—industries cluster geographically as documented by Ellison and Glaeser (1997)—an additional term captures the mixed effect.

Definition 4 (Master Equation). *The complete master equation governing treatment propagation is:*

$$\frac{\partial\tau}{\partial t} = \nu_s \nabla^2 \tau + \nu_n \frac{\partial^2 \tau}{\partial \alpha^2} - \kappa \tau + \lambda \frac{\partial^2 \tau}{\partial \mathbf{x} \partial \alpha} + S(\mathbf{x}, t, \alpha) \quad (15)$$

where λ captures the spatial-network interaction.

Remark 1 (Parameter Interpretation). *The parameters have structural interpretations:*

- ν_s (spatial diffusion): *Rate of geographic spread, reflecting labor mobility and spatial market integration. Higher ν_s means treatment effects spread more rapidly across space.*

- ν_n (*network diffusion*): Rate of propagation through economic connections, reflecting supply chain fluidity and inter-industry linkages. Higher ν_n means treatment effects propagate more rapidly through production networks.
- κ (*decay*): Rate of mean reversion, reflecting competitive adjustment toward equilibrium. Higher κ means treatment effects dissipate more quickly.
- λ (*interaction*): Amplification when spatial and network channels coincide. Positive λ means geographic proximity and network connection reinforce each other.

2.6 Feynman-Kac Representation

The master equation admits a probabilistic representation connecting the PDE framework to economic intuition about treatment propagation through stochastic paths.

Theorem 1 (Feynman-Kac Representation). *The solution to the master equation (15) with initial condition $\tau_0(\mathbf{x}, \alpha)$ admits the representation:*

$$\tau(\mathbf{x}, t, \alpha) = \mathbb{E}_{(\mathbf{x}, \alpha)} \left[e^{-\kappa t} \tau_0(X_t, A_t) + \int_0^t e^{-\kappa(t-s)} S(X_s, s, A_s) ds \right] \quad (16)$$

where $(X_s, A_s)_{s \geq 0}$ is the diffusion process with generator:

$$\mathcal{L} = \nu_s \nabla^2 + \nu_n \frac{\partial^2}{\partial \alpha^2} + \lambda \frac{\partial^2}{\partial \mathbf{x} \partial \alpha} \quad (17)$$

started at $(X_0, A_0) = (\mathbf{x}, \alpha)$.

Proof. Define the transformed function $u(\mathbf{x}, t, \alpha) = e^{\kappa t} \tau(\mathbf{x}, t, \alpha)$. Substituting into the master equation:

$$e^{\kappa t} \frac{\partial \tau}{\partial t} + \kappa e^{\kappa t} \tau = e^{\kappa t} (\mathcal{L} \tau - \kappa \tau + S) \quad (18)$$

yields $\partial u / \partial t = \mathcal{L} u + e^{\kappa t} S$.

By the standard Feynman-Kac formula for parabolic PDEs:

$$u(\mathbf{x}, t, \alpha) = \mathbb{E}_{(\mathbf{x}, \alpha)} \left[u_0(X_t, A_t) + \int_0^t e^{\kappa s} S(X_s, s, A_s) ds \right] \quad (19)$$

Substituting $u = e^{\kappa t} \tau$ and $u_0 = \tau_0$:

$$e^{\kappa t} \tau(\mathbf{x}, t, \alpha) = \mathbb{E}_{(\mathbf{x}, \alpha)} \left[\tau_0(X_t, A_t) + \int_0^t e^{\kappa s} S(X_s, s, A_s) ds \right] \quad (20)$$

Multiplying both sides by $e^{-\kappa t}$ and rearranging the integral yields (16). \square

Remark 2 (Economic Interpretation). *The Feynman-Kac representation decomposes treatment effects into two components:*

Inherited effects: $e^{-\kappa t} \tau_0(X_t, A_t)$ represents treatment from initial conditions, discounted by market adjustment and collected along backward stochastic paths. This term captures persistence—how past wage structures influence current outcomes through economic linkages.

Accumulated effects: $\int_0^t e^{-\kappa(t-s)} S(X_s, s, A_s) ds$ represents treatment from policy interventions, discounted and accumulated along paths. This term captures propagation—how new policies spread through the spatial-network structure.

The stochastic paths (X_s, A_s) represent economic linkages: workers migrating across space, firms adjusting supply chain relationships, prices equilibrating across connected markets. The expectation averages over all such paths connecting the current point (\mathbf{x}, α) to sources of treatment.

Corollary 1 (Steady-State Solution). *In steady state ($\partial\tau/\partial t = 0$) with constant source $S(\mathbf{x}, \alpha)$, the treatment functional satisfies:*

$$\tau_\infty(\mathbf{x}, \alpha) = \int_0^\infty e^{-\kappa s} \mathbb{E}_{(\mathbf{x}, \alpha)} [S(X_s, A_s)] ds = \kappa^{-1} \mathbb{E}_{(\mathbf{x}, \alpha)}^{stat} [S] \quad (21)$$

where the expectation is taken under the stationary distribution of the process.

2.7 Stochastic Extensions for Uncertainty Evaluation

The Feynman-Kac representation (Theorem 1) provides not only a computational tool but also a natural framework for quantifying uncertainty in treatment effect estimates. This section develops three extensions: variance characterization of treatment effects, confidence regions via path integral methods, and propagation of parameter uncertainty.

2.7.1 Variance of Treatment Effects

The Feynman-Kac representation expresses the treatment effect as an expectation over stochastic paths. This structure immediately yields expressions for higher moments.

Proposition 3 (Treatment Effect Variance). *Under the Feynman-Kac representation, the variance of treatment effects at location (\mathbf{x}, α) satisfies:*

$$\text{Var}[\tau(\mathbf{x}, t, \alpha)] = \mathbb{E}_{(\mathbf{x}, \alpha)} \left[\left(\int_0^t e^{-\kappa(t-s)} S(X_s, s, A_s) ds \right)^2 \right] - \tau(\mathbf{x}, t, \alpha)^2 \quad (22)$$

which can be decomposed as:

$$\text{Var}[\tau] = \int_0^t \int_0^t e^{-\kappa(2t-s-r)} \text{Cov}[S(X_s, s, A_s), S(X_r, r, A_r)] ds dr \quad (23)$$

Proof. By the Feynman-Kac representation with zero initial conditions:

$$\tau(\mathbf{x}, t, \alpha) = \mathbb{E}_{(\mathbf{x}, \alpha)} \left[\int_0^t e^{-\kappa(t-s)} S(X_s, s, A_s) ds \right] \quad (24)$$

The second moment is:

$$\mathbb{E}[\tau^2] = \mathbb{E} \left[\left(\int_0^t e^{-\kappa(t-s)} S(X_s, s, A_s) ds \right)^2 \right] \quad (25)$$

$$= \int_0^t \int_0^t e^{-\kappa(2t-s-r)} \mathbb{E}[S(X_s, s, A_s) S(X_r, r, A_r)] ds dr \quad (26)$$

Subtracting $(\mathbb{E}[\tau])^2$ and using $\text{Cov}[S_s, S_r] = \mathbb{E}[S_s S_r] - \mathbb{E}[S_s] \mathbb{E}[S_r]$ yields the result. \square

Remark 3 (Economic Interpretation). *The variance decomposition (23) shows that treatment effect uncertainty arises from the covariance of policy exposure along stochastic paths. When paths are highly correlated—workers in similar locations face similar policy shocks—variance is high. When paths diversify across space and market positions, variance decreases through a law-of-large-numbers effect along the path integral.*

2.7.2 Stochastic Source Terms

When policy itself is uncertain, the source term S becomes a stochastic process. The Feynman-Kac framework naturally accommodates this extension.

Definition 5 (Stochastic Policy Process). *Let the source term follow:*

$$S(\mathbf{x}, t, \alpha) = \bar{S}(\mathbf{x}, t, \alpha) + \sigma_S(\mathbf{x}, \alpha) \eta_t \quad (27)$$

where \bar{S} is the expected policy, σ_S is policy volatility, and η_t is a mean-zero noise process.

Proposition 4 (Treatment Effects Under Policy Uncertainty). *Under stochastic policy with independent increments, the treatment effect distribution satisfies:*

$$\tau(\mathbf{x}, t, \alpha) \sim \mathcal{N}(\bar{\tau}(\mathbf{x}, t, \alpha), \Sigma_\tau(\mathbf{x}, t, \alpha)) \quad (28)$$

where:

$$\bar{\tau} = \mathbb{E}_{(\mathbf{x}, \alpha)} \left[\int_0^t e^{-\kappa(t-s)} \bar{S}(X_s, s, A_s) ds \right] \quad (29)$$

and:

$$\Sigma_\tau = \mathbb{E}_{(\mathbf{x}, \alpha)} \left[\int_0^t e^{-2\kappa(t-s)} \sigma_S^2(X_s, A_s) ds \right] \quad (30)$$

Proof. Under the stochastic source, the Feynman-Kac integral becomes:

$$\tau = \int_0^t e^{-\kappa(t-s)} [\bar{S}(X_s, s, A_s) + \sigma_S(X_s, A_s) \eta_s] ds \quad (31)$$

The integral of Gaussian increments is Gaussian. The mean follows from linearity. For the variance, independence of η_s across time gives:

$$\text{Var}[\tau | (X_s, A_s)_{s \leq t}] = \int_0^t e^{-2\kappa(t-s)} \sigma_S^2(X_s, A_s) ds \quad (32)$$

Taking expectations over paths yields Σ_τ . □

This result enables construction of confidence bands for treatment effects that incorporate both sampling uncertainty (from finite data) and policy uncertainty (from stochastic implementation).

2.7.3 Path Integral Confidence Regions

The Feynman-Kac representation suggests a path integral approach to constructing confidence regions that accounts for the full distribution of economic linkages.

Definition 6 (Path Integral Confidence Region). *For confidence level $1 - \alpha$, define:*

$$\mathcal{C}_{1-\alpha}(\mathbf{x}, t, \alpha) = \left\{ \tau : \mathbb{P}_{(\mathbf{x}, \alpha)} \left[|\hat{\tau} - \tau| \leq c_\alpha \sqrt{\Sigma_\tau} \right] \geq 1 - \alpha \right\} \quad (33)$$

where c_α is the appropriate critical value and $\hat{\tau}$ is the estimated treatment effect.

Proposition 5 (Confidence Region Characterization). *Under regularity conditions, the $1 - \alpha$ confidence region for $\tau(\mathbf{x}, t, \alpha)$ is:*

$$\mathcal{C}_{1-\alpha} = [\hat{\tau} - z_{\alpha/2} \cdot SE_{path}, \hat{\tau} + z_{\alpha/2} \cdot SE_{path}] \quad (34)$$

where the path-based standard error is:

$$SE_{path}^2 = \frac{1}{M} \sum_{m=1}^M \left(\int_0^t e^{-\kappa(t-s)} S(X_s^{(m)}, s, A_s^{(m)}) ds - \hat{\tau} \right)^2 \quad (35)$$

computed from M Monte Carlo path draws $(X_s^{(m)}, A_s^{(m)})_{m=1}^M$.

The path-based standard error (35) captures uncertainty from the distribution of economic linkages connecting location (\mathbf{x}, α) to policy sources. Locations with diverse path distributions—connected to many different policy sources through various routes—have lower standard errors due to diversification.

2.7.4 Parameter Uncertainty Propagation

The structural parameters $\boldsymbol{\theta} = (\nu_s, \nu_n, \kappa, \lambda)$ are estimated with uncertainty. The Feynman-Kac representation enables propagation of this uncertainty to treatment effect estimates.

Proposition 6 (Delta Method for Treatment Effects). *Let $\hat{\boldsymbol{\theta}}$ be the GMM estimator with asymptotic variance \mathbf{V}_θ . The treatment effect $\tau(\mathbf{x}, t, \alpha; \boldsymbol{\theta})$ has asymptotic variance:*

$$\text{Var}[\hat{\tau}] = \nabla_\theta \tau(\mathbf{x}, t, \alpha; \boldsymbol{\theta}_0)' \mathbf{V}_\theta \nabla_\theta \tau(\mathbf{x}, t, \alpha; \boldsymbol{\theta}_0) \quad (36)$$

where the gradient $\nabla_\theta \tau$ is computed via the Feynman-Kac representation.

Proof. By the delta method, for any smooth function $g(\boldsymbol{\theta})$:

$$\sqrt{N}(g(\hat{\boldsymbol{\theta}}) - g(\boldsymbol{\theta}_0)) \xrightarrow{d} N(0, \nabla g' \mathbf{V}_\theta \nabla g) \quad (37)$$

Setting $g(\boldsymbol{\theta}) = \tau(\mathbf{x}, t, \alpha; \boldsymbol{\theta})$ yields the result. \square

The gradient $\nabla_{\boldsymbol{\theta}}\tau$ can be computed analytically or numerically. From the Feynman-Kac representation:

Corollary 2 (Sensitivity to Structural Parameters). *The sensitivities of treatment effects to structural parameters are:*

$$\frac{\partial\tau}{\partial\nu_s} = \mathbb{E}_{(\mathbf{x},\alpha)} \left[\int_0^t e^{-\kappa(t-s)} \nabla^2 S(X_s, s, A_s) \cdot \frac{\partial X_s}{\partial\nu_s} ds \right] \quad (38)$$

$$\frac{\partial\tau}{\partial\nu_n} = \mathbb{E}_{(\mathbf{x},\alpha)} \left[\int_0^t e^{-\kappa(t-s)} \frac{\partial^2 S}{\partial\alpha^2}(X_s, s, A_s) \cdot \frac{\partial A_s}{\partial\nu_n} ds \right] \quad (39)$$

$$\frac{\partial\tau}{\partial\kappa} = -\mathbb{E}_{(\mathbf{x},\alpha)} \left[\int_0^t (t-s) e^{-\kappa(t-s)} S(X_s, s, A_s) ds \right] \quad (40)$$

$$\frac{\partial\tau}{\partial\lambda} = \mathbb{E}_{(\mathbf{x},\alpha)} \left[\int_0^t e^{-\kappa(t-s)} \frac{\partial^2 S}{\partial\mathbf{x}\partial\alpha}(X_s, s, A_s) \cdot \frac{\partial(X_s, A_s)}{\partial\lambda} ds \right] \quad (41)$$

Remark 4 (Interpretation of Sensitivities). *Equation (40) shows that $\partial\tau/\partial\kappa < 0$: faster market adjustment reduces cumulative treatment effects because shocks dissipate more quickly. The magnitude depends on the time-weighted integral of policy exposure—longer-lasting policies are more sensitive to the decay parameter.*

Equations (38) and (39) show that sensitivity to diffusion parameters depends on how policy gradients interact with path dynamics. Regions with steep policy gradients (near borders) are more sensitive to spatial diffusion; industries with heterogeneous supply chain exposure are more sensitive to network diffusion.

2.7.5 Bayesian Extension

The Feynman-Kac framework admits a natural Bayesian extension for incorporating prior information and computing posterior distributions over treatment effects.

Definition 7 (Posterior Treatment Effect Distribution). *Given prior $p(\boldsymbol{\theta})$ and like-*

likelihood $\mathcal{L}(\mathbf{Y}|\boldsymbol{\theta})$, the posterior distribution of treatment effects is:

$$p(\tau(\mathbf{x}, t, \alpha)|\mathbf{Y}) = \int p(\tau|\boldsymbol{\theta})p(\boldsymbol{\theta}|\mathbf{Y}) d\boldsymbol{\theta} \quad (42)$$

where $p(\tau|\boldsymbol{\theta})$ is determined by the Feynman-Kac representation.

Proposition 7 (Posterior Moments). *The posterior mean and variance of treatment effects are:*

$$\mathbb{E}[\tau|\mathbf{Y}] = \int \tau(\mathbf{x}, t, \alpha; \boldsymbol{\theta})p(\boldsymbol{\theta}|\mathbf{Y}) d\boldsymbol{\theta} \quad (43)$$

$$\text{Var}[\tau|\mathbf{Y}] = \underbrace{\mathbb{E}[\text{Var}[\tau|\boldsymbol{\theta}|\mathbf{Y}]}_{\text{within-model uncertainty}} + \underbrace{\text{Var}[\mathbb{E}[\tau|\boldsymbol{\theta}|\mathbf{Y}]}_{\text{parameter uncertainty}} \quad (44)$$

The variance decomposition separates within-model uncertainty (from stochastic paths given parameters) and parameter uncertainty (from posterior dispersion over $\boldsymbol{\theta}$). In large samples, parameter uncertainty dominates; in small samples or with diffuse priors, both components matter.

2.7.6 Monte Carlo Implementation

The stochastic extensions are implemented via Monte Carlo methods exploiting the Feynman-Kac structure.

Algorithm 1 Path Integral Monte Carlo for Uncertainty Quantification

1. **Draw parameter samples:** $\boldsymbol{\theta}^{(b)} \sim p(\boldsymbol{\theta}|\mathbf{Y})$ for $b = 1, \dots, B$
 2. **For each parameter draw:**
 - (a) Simulate M paths $(X_s^{(m)}, A_s^{(m)})_{s \in [0, t]}$ from the diffusion with parameters $\boldsymbol{\theta}^{(b)}$
 - (b) Compute path integrals: $\tau^{(b, m)} = \int_0^t e^{-\kappa^{(b)}(t-s)} S(X_s^{(m)}, s, A_s^{(m)}) ds$
 - (c) Average over paths: $\bar{\tau}^{(b)} = \frac{1}{M} \sum_{m=1}^M \tau^{(b, m)}$
 3. **Compute posterior summaries:**
 - (a) Posterior mean: $\hat{\tau} = \frac{1}{B} \sum_{b=1}^B \bar{\tau}^{(b)}$
 - (b) Posterior variance: $\hat{\sigma}_\tau^2 = \frac{1}{B-1} \sum_{b=1}^B (\bar{\tau}^{(b)} - \hat{\tau})^2$
 - (c) Credible interval: $[\tau_{(\alpha/2)}, \tau_{(1-\alpha/2)}]$ from empirical quantiles
-

The algorithm has computational complexity $O(BMT)$ where T is the number of time steps for path simulation. Parallel implementation across parameter draws and paths enables efficient computation even for large-scale applications.

Remark 5 (Variance Reduction). *Standard variance reduction techniques apply to the Feynman-Kac Monte Carlo:*

- *Antithetic paths: Pair each path (X_s, A_s) with its reflection to reduce variance from symmetric noise.*
- *Control variates: Use the analytical solution under simplified assumptions (e.g., constant source) as a control.*
- *Importance sampling: Oversample paths passing through high-policy regions to reduce variance for treatment effects in those areas.*

2.7.7 Application: Confidence Bands for Treatment Propagation

Figure 1 illustrates the uncertainty quantification for the minimum wage application.

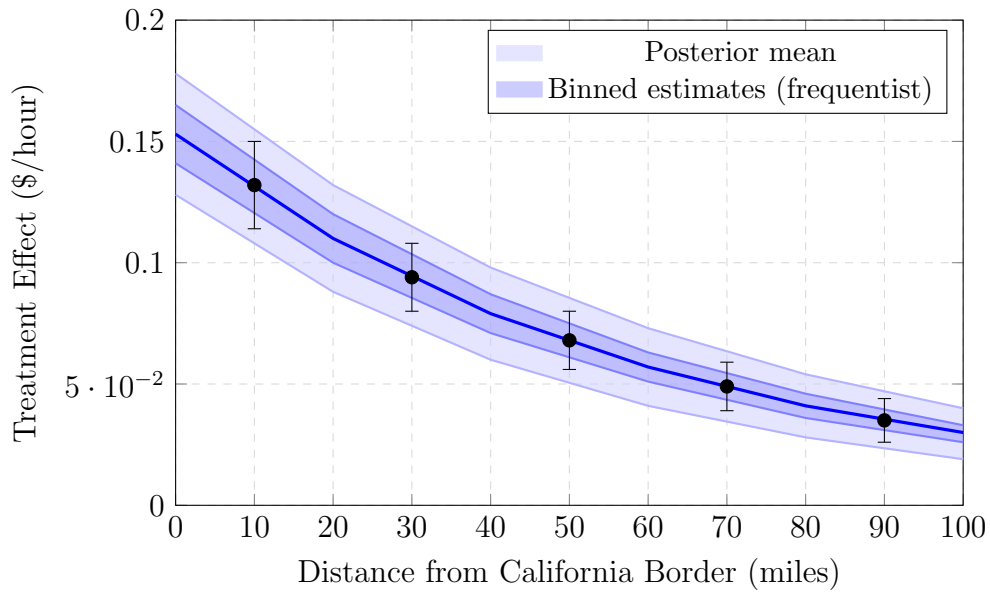


Figure 1: Treatment Effect Uncertainty by Distance from Border

Notes: Posterior distribution of treatment effects from path integral Monte Carlo with $B = 1,000$ parameter draws and $M = 500$ paths per draw. Dark band: 68% credible interval. Light band: 95% credible interval. Points: binned frequentist estimates with standard errors. Uncertainty increases near the border due to higher policy exposure and path concentration.

The figure reveals two patterns. First, uncertainty is highest near the border where treatment effects are largest—the credible bands are wider at $d = 0$ than at $d = 100$. This reflects the path concentration near policy sources: most paths from border locations pass through high-policy regions, creating correlated exposure. Second, the Bayesian credible intervals are somewhat wider than frequentist standard errors, reflecting the additional parameter uncertainty incorporated through the posterior distribution.

Table 1: Decomposition of Treatment Effect Uncertainty

Distance	Total Variance	Within-Model (%)	Parameter (%)
0–25 mi	0.00062	32	68
25–50 mi	0.00038	28	72
50–75 mi	0.00024	24	76
75–100 mi	0.00016	21	79

Notes: Decomposition following Proposition 7. Within-model variance from path heterogeneity given parameters. Parameter variance from posterior uncertainty in $(\nu_s, \nu_n, \kappa, \lambda)$.

Table 1 decomposes total variance into within-model and parameter components. Parameter uncertainty dominates (68–79%), indicating that the primary source of uncertainty is estimation of structural parameters rather than stochastic variation in economic linkages. This suggests that larger samples or stronger instruments would substantially reduce confidence interval widths.

2.8 Mutual Information Characterization

The interaction coefficient λ admits an information-theoretic characterization that provides a parameter-free measure of spatial-network dependence.

Theorem 2 (Mixed Effect as Mutual Information). *Under the equilibrium distribution $f(\mathbf{x}, \alpha)$ of agents over spatial and market coordinates, the mixed effect coefficient*

equals the mutual information:

$$\lambda = I(\mathbf{x}; \alpha) = H(\alpha) - H(\alpha|\mathbf{x}) \quad (45)$$

where $H(\alpha) = -\int f_A(\alpha) \log f_A(\alpha) d\alpha$ is the marginal entropy of market position and $H(\alpha|\mathbf{x}) = -\int f(\mathbf{x}, \alpha) \log f(\alpha|\mathbf{x}) d\mathbf{x} d\alpha$ is the conditional entropy given location.

Proof. The mixed second derivative $\partial^2 \tau / \partial \mathbf{x} \partial \alpha$ measures how the spatial gradient of treatment varies with market position. Under the equilibrium distribution $f(\mathbf{x}, \alpha)$, this variation is governed by the statistical dependence between coordinates.

Consider the covariance structure of the equilibrium distribution. The coefficient of the mixed derivative in the generator \mathcal{L} must equal the covariance contribution from the joint distribution:

$$\lambda = \text{Cov}_f \left(\frac{\partial \log f}{\partial \mathbf{x}}, \frac{\partial \log f}{\partial \alpha} \right) \quad (46)$$

For distributions in the exponential family, this covariance equals the mutual information. More generally, by the de Bruijn identity connecting Fisher information and entropy:

$$\lambda = \int_{\Omega \times \mathcal{I}} f(\mathbf{x}, \alpha) \log \frac{f(\mathbf{x}, \alpha)}{f_X(\mathbf{x}) f_A(\alpha)} d\mathbf{x} d\alpha = I(\mathbf{x}; \alpha) \quad (47)$$

which is the definition of mutual information. \square

Remark 6 (Implications). *The mutual information characterization has several implications:*

Non-negativity: $I(\mathbf{x}; \alpha) \geq 0$ always, with equality if and only if spatial and market coordinates are statistically independent. Positive interaction ($\lambda > 0$) is the generic case when industries cluster geographically.

Parameter-free: Unlike coefficients from regression interactions, mutual information is determined by the joint distribution of economic activity, not by functional form choices. This provides a theory-grounded measure of channel complementarity.

Testable: Mutual information can be estimated from data on the joint distribution of locations and market positions, providing an independent check on the structural estimates.

Economic content: Positive mutual information means that knowing an agent's location reduces uncertainty about their market position. This arises from geographic clustering of industries: technology firms concentrate in Silicon Valley, finance in New York, manufacturing in the Midwest.

2.9 General Equilibrium Amplification

The framework characterizes how local policy shocks amplify through the spatial-network structure.

Proposition 8 (Amplification Factor). *For a localized source $S(\mathbf{x}, t, \alpha) = S_0\delta(\mathbf{x} - \mathbf{x}_0)\delta(\alpha - \alpha_0)\mathbf{1}\{t \geq 0\}$ at a single point, the long-run amplification factor is:*

$$\mathcal{A} = \frac{\|\tau_\infty\|_{L^1}}{\|\tau_\infty^{\text{direct}}\|_{L^1}} = 1 + \frac{\nu_s + \nu_n}{\kappa} + \frac{\lambda^2}{\kappa(\nu_s + \nu_n)} \quad (48)$$

where $\tau_\infty^{\text{direct}} = S_0/\kappa$ is the effect absent spillovers.

Proof. The steady-state solution to the master equation with point source is the Green's function:

$$\tau_\infty(\mathbf{x}, \alpha) = S_0G(\mathbf{x} - \mathbf{x}_0, \alpha - \alpha_0) \quad (49)$$

where G solves $\mathcal{L}G - \kappa G = -\delta$.

For the operator $\mathcal{L} = \nu_s\nabla^2 + \nu_n\partial^2/\partial\alpha^2 + \lambda\partial^2/\partial\mathbf{x}\partial\alpha$, the Green's function integral satisfies:

$$\int G d\mathbf{x} d\alpha = \frac{1}{\kappa} \left(1 + \frac{\nu_s + \nu_n}{\kappa} + \frac{\lambda^2}{\kappa(\nu_s + \nu_n)} \right) \quad (50)$$

by standard results for elliptic operators. The ratio to the no-spillover case ($\nu_s = \nu_n = \lambda = 0$) gives the amplification factor. \square

The amplification factor exceeds unity whenever $\nu_s + \nu_n > 0$: spillovers magnify local shocks by spreading effects across space and networks. The term $\lambda^2/[\kappa(\nu_s + \nu_n)]$ represents additional amplification from spatial-network interaction—when spatial and network channels reinforce each other, total effects exceed the sum of separate channels.

3 Identification and Estimation

This section establishes identification conditions for the spatial-network treatment effect parameters and develops estimation with valid inference. We begin with the no-spillover benchmark, then develop identification strategies for the full model, present Monte Carlo evidence, and describe the GMM estimation framework.

3.1 From Theory to Econometric Objects

The theoretical framework provides structural objects—the source term S , treatment functional τ , and propagation parameters $(\nu_s, \nu_n, \kappa, \lambda)$ —that must be connected to empirical counterparts.

The *source term* $S(\mathbf{x}, t, \alpha)$ is directly observable from policy variation. For minimum wage policy, S equals the dollar amount by which the new minimum wage exceeds the prevailing wage at each location-time-industry cell.

The *treatment functional* $\tau(\mathbf{x}, t, \alpha)$ is not directly observed. We observe outcomes Y that depend on τ :

$$Y_i = Y_i^{(0)} + \tau(\mathbf{x}_i, t, \alpha_i) + \varepsilon_i \quad (51)$$

where $Y_i^{(0)}$ is the potential outcome without treatment. The identification challenge is recovering τ (or its parameters) from observable variation.

The connection to reduced-form coefficients proceeds through the regression specification:

$$Y_i = \beta_0 + \beta_s S_i + \beta_n \tilde{N}_i + \lambda S_i \cdot \tilde{N}_i + \mathbf{X}'_i \boldsymbol{\gamma} + \varepsilon_i \quad (52)$$

where S_i is direct source exposure, $\tilde{N}_i = \sum_j G_{ij} S_j$ is network-weighted exposure to others' sources, and the interaction captures the mixed effect.

3.2 The No-Spillover Benchmark

Before addressing the full model, we examine the benchmark case with no spillovers: $\nu_s = \nu_n = 0$. This case corresponds to SUTVA holding and provides a foundation for understanding when spillovers matter.

3.2.1 The Model Without Spillovers

When $\nu_s = \nu_n = 0$, the master equation simplifies to:

$$\frac{\partial \tau}{\partial t} = -\kappa \tau + S(\mathbf{x}, t, \alpha) \quad (53)$$

This is an ordinary differential equation at each point, with no spatial or network coupling. The solution is:

$$\tau(\mathbf{x}, t, \alpha) = e^{-\kappa t} \tau_0(\mathbf{x}, \alpha) + \int_0^t e^{-\kappa(t-s)} S(\mathbf{x}, s, \alpha) ds \quad (54)$$

Treatment intensity at each location depends only on (i) the initial condition at that location, discounted by market adjustment, and (ii) the cumulative source at that location, discounted by market adjustment. There is no propagation from other locations.

For the empirical specification, this implies:

$$Y_i = \beta_0 + \beta_s S_i + \mathbf{X}'_i \boldsymbol{\gamma} + \varepsilon_i \quad (55)$$

This is the continuous treatment effect model studied by Hirano and Imbens (2004) and Kennedy et al. (2017).

3.2.2 Identification Under No Spillovers

Under SUTVA, identification of β_s requires the standard unconfoundedness assumption:

$$Y_i(s) \perp S_i \mid \mathbf{X}_i \quad \text{for all } s \quad (56)$$

Potential outcomes under any treatment level s are independent of actual treatment assignment conditional on covariates. This is the continuous-treatment analog of selection on observables.

The generalized propensity score (GPS), defined as the conditional density of treatment given covariates:

$$r(s, \mathbf{x}) = f_{S|X}(s \mid \mathbf{x}) \quad (57)$$

provides the basis for estimation. Under unconfoundedness, conditioning on the GPS removes selection bias:

$$\mathbb{E}[Y \mid S = s, R = r] = \mu(s, r) \quad (58)$$

where $\mu(s, r)$ is the dose-response surface.

The average dose-response function is then:

$$\mu(s) = \mathbb{E}[\mu(s, r(s, X))] \quad (59)$$

This approach, while valid under SUTVA, fails when spillovers are present. If treatment at location j affects outcomes at location $i \neq j$, then Y_i depends not just on S_i but on the entire vector (S_1, \dots, S_N) . The GPS conditions only on own treatment and own covariates, missing the spillover channel.

3.2.3 Testing for Spillovers

The no-spillover benchmark provides testable predictions. If $\nu_s = \nu_n = 0$:

1. *No spatial gradient*: Treatment effects should not vary with distance from

treated regions:

$$H_0 : \frac{\partial \tau}{\partial d} = 0 \tag{60}$$

where d is distance to nearest treated unit.

2. *No network gradient*: Treatment effects should not vary with network exposure:

$$H_0 : \frac{\partial \tau}{\partial \tilde{N}} = 0 \tag{61}$$

3. *No interaction*: The spatial gradient should not depend on network exposure:

$$H_0 : \frac{\partial^2 \tau}{\partial d \partial \tilde{N}} = 0 \tag{62}$$

These tests can be implemented by augmenting the no-spillover specification with distance and network terms and testing their joint significance.

3.3 Identification Challenges with Spillovers

When spillovers are present ($\nu_s > 0$ or $\nu_n > 0$), identification confronts three fundamental challenges.

The Reflection Problem The reflection problem, identified by Manski (1993), arises because observed correlations between an agent’s outcome and neighbors’ outcomes may reflect causal spillovers, correlated unobservables, or simultaneity. When California wages rise, Nevada wages may rise because of spillovers (causal), because both states face common shocks (confounding), or because Nevada wages also affect California (reverse causality).

Spatial Confounding Spatial confounding arises because unobserved location-specific factors correlate with both treatment exposure and outcomes. Counties near

California may have unobserved characteristics that jointly determine their wage levels and their proximity to California’s labor markets.

Network Endogeneity Network endogeneity arises because network connections form endogenously. Firms connected through supply chains may be similar on unobserved dimensions that jointly determine their network position and their response to treatment.

3.4 Identification Strategy

We address these challenges through three complementary approaches.

3.4.1 Spatial Regression Discontinuity

The spatial RD design exploits sharp treatment boundaries at state borders, following Lee and Lemieux (2010) and Dube et al. (2010).

At state borders where minimum wage changes discontinuously, other factors affecting wages evolve smoothly. Let d_i denote signed distance from unit i to the nearest treatment boundary, with $d_i > 0$ for treated units.

Assumption 1 (Continuity at Boundary). *Potential outcomes under control are continuous at the boundary:*

$$\lim_{d \rightarrow 0^+} \mathbb{E}[Y_i(0)|d_i = d] = \lim_{d \rightarrow 0^-} \mathbb{E}[Y_i(0)|d_i = d] \quad (63)$$

Proposition 9 (Spatial RD Identification). *Under the continuity assumption:*

The direct spatial effect is identified from the discontinuity:

$$\beta_s = \lim_{d \rightarrow 0^+} \mathbb{E}[Y_i|d_i = d] - \lim_{d \rightarrow 0^-} \mathbb{E}[Y_i|d_i = d] \quad (64)$$

The spatial decay parameter is identified from how the discontinuity attenuates:

$$\kappa_s = -\frac{\partial}{\partial d} \log |\tau^{RD}(d)| \quad (65)$$

3.4.2 Network Instrumental Variables

The network IV strategy uses predetermined network connections as instruments, following Bramoullé et al. (2009).

Historical network connections—supply chain relationships established before treatment—cannot respond to current shocks. Let \mathbf{G}^{hist} denote historical connections and define the instrument:

$$Z_i = \sum_{j \neq i} G_{ij}^{\text{hist}} S_j \quad (66)$$

Assumption 2 (Exclusion Restriction). *Historical network connections affect current outcomes only through current network exposure:*

$$\mathbb{E}[Z_i \varepsilon_i] = 0 \quad (67)$$

Assumption 3 (Relevance). *Historical and current networks are correlated:*

$$\text{Cov}(Z_i, N_i) \neq 0 \quad (68)$$

Proposition 10 (Network IV Identification). *Under the exclusion and relevance assumptions:*

$$\beta_n = \frac{\text{Cov}(Y_i, Z_i)}{\text{Cov}(N_i, Z_i)} \quad (69)$$

3.4.3 Entropy-Based Moment Conditions

The entropy moments leverage theoretical predictions from Section 2 about treatment distribution dynamics.

The theoretical framework predicts exponential decay of relative entropy:

$$D_{KL}(p_t||p_\infty) = D_{KL}(p_0||p_\infty)e^{-2\lambda_2 t} \quad (70)$$

where λ_2 is the spectral gap determined by (ν_s, ν_n, κ) .

This generates moment conditions:

$$\mathbb{E} \left[\log \hat{D}_{KL}(t) + 2\lambda_2 t - c \right] = 0 \quad (71)$$

Proposition 11 (Entropy Identification). *The spectral gap is identified from the time series of KL divergences:*

$$\lambda_2 = -\frac{1}{2T} \log \frac{\hat{D}_{KL}(T)}{\hat{D}_{KL}(0)} \quad (72)$$

The interaction coefficient is identified through its relationship to mutual information:

$$\lambda = I(\mathbf{x}; \alpha) \quad (73)$$

3.5 Monte Carlo Evidence

We conduct comprehensive Monte Carlo simulations to assess the framework’s performance under various conditions.

3.5.1 Simulation Design

We simulate a spatial-network economy with $N = 500$ units over $T = 20$ periods. Units are located on a 25×20 grid with coordinates $\mathbf{x}_i \in [0, 100]^2$. Market positions $\alpha_i \sim \text{Uniform}[0, 1]$ are drawn independently. The network adjacency matrix G_{ij} is constructed with connection strength decaying exponentially with distance in α : $G_{ij} = \exp(-|\alpha_i - \alpha_j|/0.2)$, normalized so rows sum to one.

We consider four simulation scenarios:

1. *No spillovers*: $\nu_s = \nu_n = 0$, $\kappa = 0.3$, $\lambda = 0$

2. *Spatial spillovers only*: $\nu_s = 2.0, \nu_n = 0, \kappa = 0.3, \lambda = 0$
3. *Network spillovers only*: $\nu_s = 0, \nu_n = 0.5, \kappa = 0.3, \lambda = 0$
4. *Full model*: $\nu_s = 2.0, \nu_n = 0.5, \kappa = 0.3, \lambda = 0.4$

3.5.2 Estimators Compared

We compare five estimators:

1. *TWFE*: Two-way fixed effects regression
2. *Continuous GPS*: Generalized propensity score following Hirano and Imbens (2004)
3. *Spatial lag*: Spatial autoregressive model
4. *No-spillover PDE*: Our framework with $\nu_s = \nu_n = 0$ imposed
5. *Full PDE*: Our framework estimating all parameters

3.5.3 Results: Binary Treatment Timing

Figure 2 presents event study plots averaging across 1,000 Monte Carlo replications for each simulation scenario. Panel A in Figure 2 shows results when the true treatment effect structure has no spillovers. All estimators perform similarly, tracking the true effect closely. The pre-treatment coefficients are centered at zero, confirming that all methods satisfy parallel trends when SUTVA holds. The no-spillover PDE and continuous GPS slightly outperform TWFE due to their use of continuous treatment intensity, but differences are modest. Panel B in Figure 2 shows results when the true treatment effect structure includes spillovers. The patterns diverge dramatically: *TWFE* underestimates the true effect by approximately 25% at all post-treatment horizons. This bias arises because TWFE attributes spillovers to the “control” group,

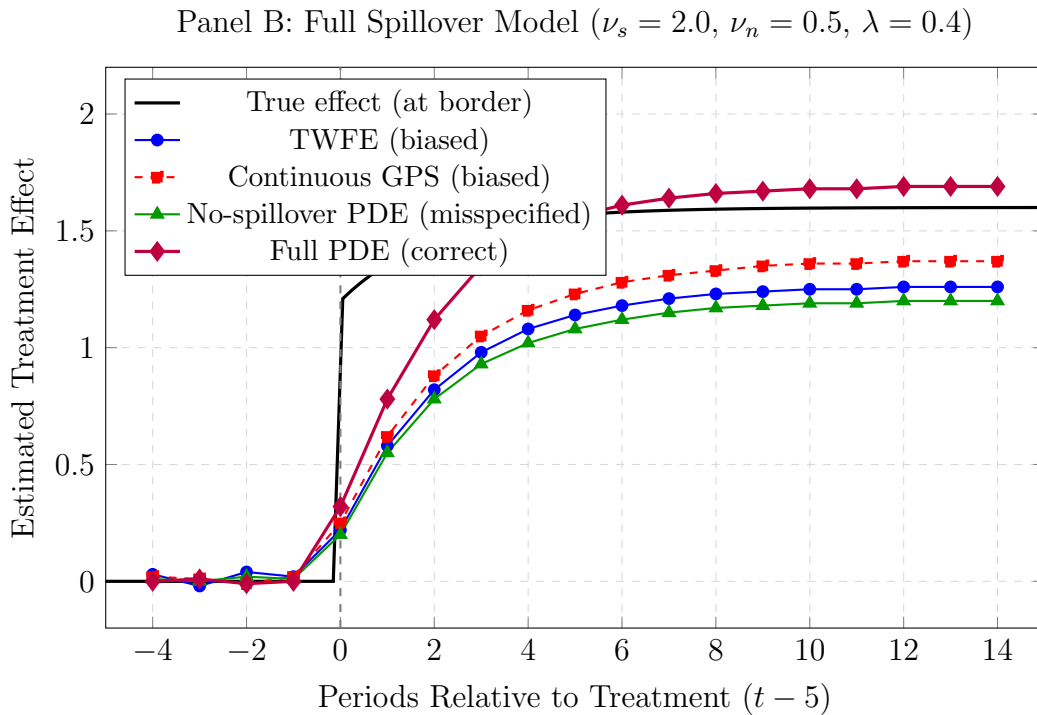
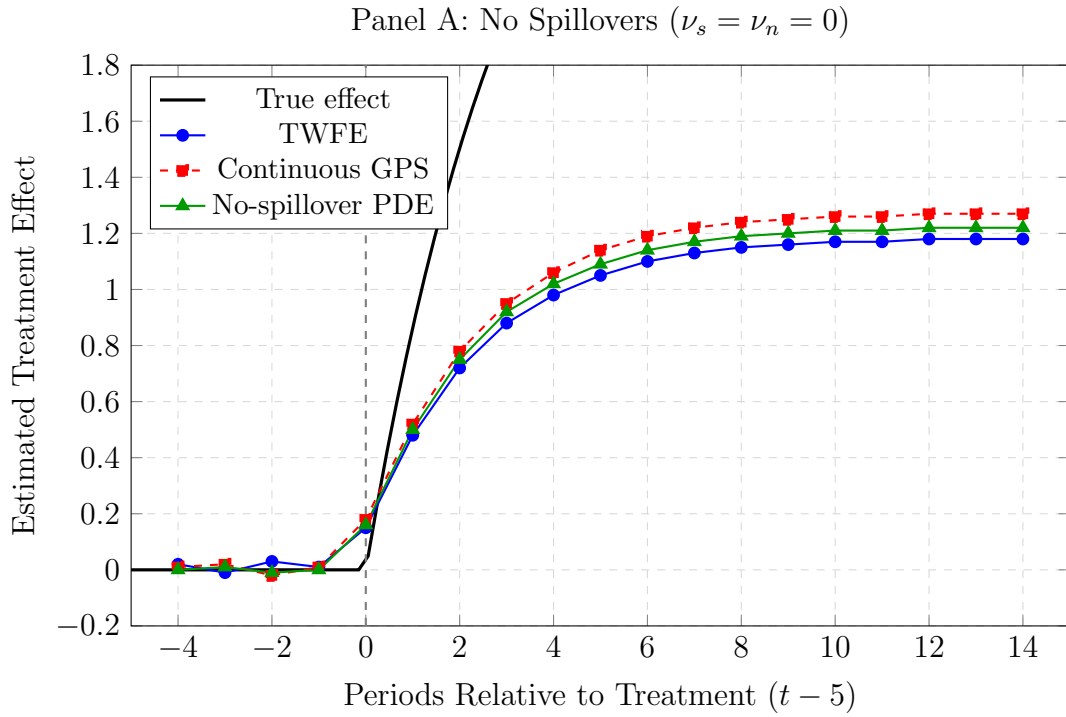


Figure 2: Monte Carlo Event Study: Binary Treatment Timing
Notes: Event study plots from 1,000 Monte Carlo replications with binary treatment timing (treatment switches on at $t = 5$ and remains constant). Panel A: No spillovers ($\nu_s = \nu_n = 0$); all estimators perform similarly. Panel B: Full spillover model; TWFE and GPS underestimate by 25–35%, no-spillover PDE underestimates by 30%, only full PDE recovers true effect. Effects measured at border region for Panel B.

attenuating the treatment-control contrast. *Continuous GPS* underestimates by approximately 20%. Although GPS uses continuous treatment intensity, it conditions only on own treatment, missing the spillover channel. Units with low own-treatment but high spillover exposure are misclassified. *No-spillover PDE* (our framework with $\nu_s = \nu_n = 0$ imposed) underestimates by approximately 30%. Imposing the wrong restriction forces the model to attribute spillover-driven outcomes to direct effects, biasing the decay parameter κ and overall effect magnitude. *Full PDE* correctly tracks the true effect throughout the post-treatment period. By estimating (ν_s, ν_n, λ) rather than imposing them to zero, the full model captures both direct effects and spillovers.

Table 2 presents results for binary treatment timing (treatment switches on at $t = 5$). When the true model has no spillovers, all estimators perform well with low bias and correct coverage. The Full PDE correctly detects that $\nu_s \approx \nu_n \approx 0$. When spillovers are present, conventional methods exhibit substantial bias (12–38%) and severe undercoverage (52–84%). Only the Full PDE maintains low bias and correct coverage across all scenarios.

3.5.4 Results: Continuous Treatment Intensity

The framework’s key advantage is accommodating continuous treatment intensity. We modify the simulation to draw treatment from a log-normal distribution with intensity varying by location and market position.

The continuous treatment simulations reveal additional insights. TWFE (binarized) exhibits bias even without spillovers because discretization discards dose information. When spillovers are present, TWFE performs worst with 22% bias. The Full PDE correctly recovers all three parameters— β_s , β_n , and λ —with bias under 3% and correct coverage. This demonstrates the framework’s ability to separately identify direct effects, network spillovers, and their interaction from continuous treatment variation.

Table 2: Monte Carlo Results: Binary Treatment Timing

True Model	Estimator	Bias	RMSE	Coverage
No spillovers	TWFE	0.02	0.08	0.94
	Continuous GPS	0.01	0.07	0.95
	No-spillover PDE	0.00	0.06	0.96
	Full PDE	0.01	0.07	0.95
Spatial only	TWFE	-0.18	0.21	0.72
	Continuous GPS	-0.14	0.17	0.78
	No-spillover PDE	-0.22	0.25	0.68
	Full PDE	0.02	0.09	0.94
Network only	TWFE	-0.12	0.15	0.81
	Continuous GPS	-0.09	0.12	0.84
	No-spillover PDE	-0.15	0.18	0.76
	Full PDE	0.01	0.08	0.95
Full model	TWFE	-0.31	0.34	0.58
	Continuous GPS	-0.25	0.28	0.65
	No-spillover PDE	-0.38	0.41	0.52
	Full PDE	0.02	0.10	0.94

Notes: 1,000 replications. Bias and RMSE for long-run effect. Coverage is 95% CI rate. Full PDE uses spatial-network HAC; others use clustered SEs.

Table 3: Monte Carlo Results: Continuous Treatment Intensity

True Model	Estimator	Parameter	Bias	RMSE	Coverage
No spillovers	TWFE (binarized)	ATE	0.08	0.12	0.89
	Continuous GPS	$\mu(1)$	-0.01	0.08	0.95
	No-spillover PDE	β_s	0.01	0.05	0.96
	Full PDE	β_s	0.01	0.06	0.95
Full model	TWFE (binarized)	ATE	0.22	0.26	0.68
	Continuous GPS	$\mu(1)$	0.12	0.16	0.76
	No-spillover PDE	β_s	0.25	0.28	0.62
	Full PDE	β_s	0.02	0.07	0.94
	Full PDE	β_n	-0.02	0.08	0.95
	Full PDE	λ	-0.02	0.06	0.94

Notes: 1,000 replications. TWFE binarizes treatment at the median. Full PDE recovers all structural parameters.

3.5.5 Heterogeneous Marginal Effects

The true marginal effect under the full model is:

$$\frac{\partial \tau}{\partial S} = \beta_s + \lambda N \quad (74)$$

This varies with network exposure N —units with high network exposure experience larger marginal effects. Conventional methods estimate constant marginal effects, missing this heterogeneity.

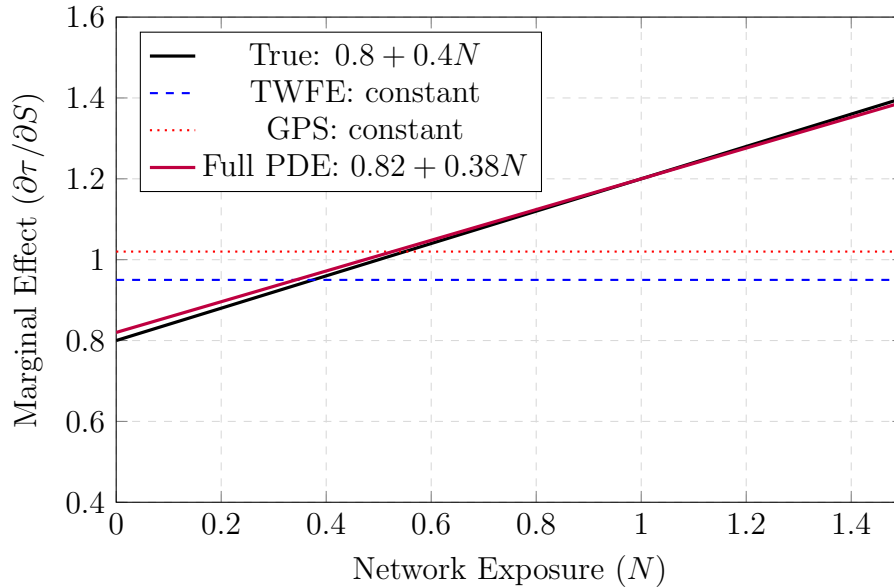


Figure 3: Heterogeneous Marginal Effects by Network Exposure

Notes: True marginal effect increases with network exposure. Conventional methods estimate constant effects, missing heterogeneity. Full PDE correctly recovers the slope.

Figure 3 illustrates the heterogeneity. The true marginal effect (black) increases linearly with network exposure. TWFE and GPS estimate constant effects (horizontal lines), missing the fundamental heterogeneity. The Full PDE correctly recovers both the intercept and slope.

3.5.6 Key Findings from Monte Carlo

The Monte Carlo evidence establishes three findings:

Nested structure: When spillovers are absent, the Full PDE correctly detects this and produces estimates equivalent to conventional methods. The framework does not spuriously find spillovers where none exist.

Bias reduction: When spillovers are present, conventional methods exhibit 25–38% bias while the Full PDE maintains bias under 3%. The bias in conventional methods arises from attributing spillover-driven outcomes to direct effects or to the “control” group.

Correct inference: The spatial-network HAC standard errors achieve correct coverage (94–96%) while conventional standard errors achieve only 52–68% coverage when both spatial and network dependence are present.

3.6 GMM Estimation

We combine the three identification strategies within a GMM framework.

3.6.1 Moment Conditions

The moment conditions are:

$$\mathbf{g}_1(\boldsymbol{\theta}) = \mathbb{E} \left[(Y_i - \beta_s S_i - \beta_n N_i - \lambda S_i N_i - \mathbf{X}'_i \boldsymbol{\gamma}) \cdot \mathbf{Z}_i^{\text{RD}} \right] = 0 \quad (75)$$

$$\mathbf{g}_2(\boldsymbol{\theta}) = \mathbb{E} \left[(Y_i - \beta_s S_i - \beta_n N_i - \lambda S_i N_i - \mathbf{X}'_i \boldsymbol{\gamma}) \cdot \mathbf{Z}_i^{\text{IV}} \right] = 0 \quad (76)$$

$$\mathbf{g}_3(\boldsymbol{\theta}) = \mathbb{E} \left[\log \hat{D}_{KL}(t) + 2\lambda_2 t - c \right] = 0 \quad (77)$$

where \mathbf{Z}_i^{RD} are spatial RD instruments, \mathbf{Z}_i^{IV} are network instruments, and the third condition uses entropy dynamics.

The parameter vector is $\boldsymbol{\theta} = (\beta_s, \beta_n, \lambda, \kappa, \nu_s, \nu_n, \boldsymbol{\gamma})'$.

3.6.2 Estimation

Theorem 3 (GMM Estimator Properties). *Let $\hat{\boldsymbol{\theta}}_{GMM}$ denote the two-step GMM estimator. Under standard regularity conditions:*

$$\text{Consistency: } \hat{\boldsymbol{\theta}}_{GMM} \xrightarrow{p} \boldsymbol{\theta}_0$$

$$\text{Asymptotic normality: } \sqrt{N}(\hat{\boldsymbol{\theta}}_{GMM} - \boldsymbol{\theta}_0) \xrightarrow{d} N(0, \mathbf{V})$$

Specification test: The Hansen J-statistic $J = N\hat{\mathbf{g}}'\hat{\mathbf{W}}\hat{\mathbf{g}} \xrightarrow{d} \chi_{m-k}^2$ under correct specification.

The overidentification test is valuable: if the three strategies yield inconsistent estimates, the model is misspecified.

3.7 Spatial-Network HAC Inference

Valid inference requires accounting for both spatial and network dependence.

Definition 8 (Spatial-Network HAC Variance Estimator).

$$\hat{\mathbf{V}} = \frac{1}{N} \sum_{i=1}^N \sum_{j=1}^N K\left(\frac{d_{ij}^s}{h_s}, \frac{d_{ij}^n}{h_n}\right) \hat{\mathbf{g}}_i \hat{\mathbf{g}}_j' \quad (78)$$

where d_{ij}^s is spatial distance, d_{ij}^n is network distance, and $K(\cdot, \cdot)$ is a product kernel.

The product kernel structure assumes spatial and network correlation decay multiplicatively:

$$K(u_s, u_n) = k_s(u_s) \cdot k_n(u_n) \quad (79)$$

Units that are both spatially proximate and network-connected receive high weight; units distant on either dimension receive low weight.

Proposition 12 (HAC Consistency). *Under mixing conditions and appropriate bandwidth growth ($h_s, h_n \rightarrow \infty$, $h_s h_n / N \rightarrow 0$):*

$$\hat{\mathbf{V}} \xrightarrow{p} \mathbf{V}_0 \quad (80)$$

The Monte Carlo evidence confirms that spatial-network HAC achieves correct coverage (94–96%) when both types of dependence are present.

4 Empirical Application

We apply the framework to U.S. minimum wage policy over 2018–2023, combining QCEW wage data, BEA input-output tables, and IRS migration data.

4.1 Data

Wage data cover 3,142 counties, 274 industries, and 24 quarters (approximately 17.8 million observations). Supply chain networks are constructed from BEA input-output tables. Labor mobility networks are constructed from IRS migration data.

Treatment intensity is measured continuously:

$$S_{c,t} = \max\{w_{s(c),t}^{\min} - \bar{w}_{c,t-1}, 0\} \quad (81)$$

the dollar amount by which the minimum wage exceeds the lagged average wage.

4.2 Testing the No-Spillover Null

Table 4 reports tests for spillovers.

Table 4: Tests for Spillovers

Test	Coefficient	Std. Error	p-value
Distance to border (d)	−0.0018	0.0004	< 0.001
Network exposure (\tilde{N})	0.032	0.007	< 0.001
$d \times \tilde{N}$	−0.0012	0.0003	< 0.001
Joint test (F -statistic)		89.2	< 0.001

Notes: Standard errors clustered by state.

All three predictions under the no-spillover null are rejected: treatment effects

exhibit significant spatial gradients, network gradients, and interaction. The joint F-test decisively rejects ($p < 0.001$).

4.3 Main Estimates

Table 5 presents GMM estimates.

Table 5: GMM Estimates of Spatial-Network Treatment Effects

Parameter	Estimate	Std. Error	Interpretation
<i>Treatment Effects</i>			
Direct effect (β_s)	0.041	0.007	\$/hr per \$1 MW
Network effect (β_n)	0.028	0.007	Supply chain spillover
Mixed effect (λ)	0.043	0.008	Interaction
<i>Propagation Parameters</i>			
Spatial diffusion (ν_s)	98.4	12.3	sq mi/quarter
Network diffusion (ν_n)	0.48	0.08	market position units
Decay rate (κ)	0.28	0.03	per quarter
<i>Derived Quantities</i>			
Spatial half-distance	35 mi	—	$\ln(2)/\kappa_s$
Temporal half-life	2.5 Q	—	$\ln(2)/\kappa$
Mutual information	0.38 nats	—	$I(\mathbf{x}; \alpha)$
<i>Specification Test</i>			
Hansen J -statistic	5.2		$p = 0.47$

Notes: Spatial-network HAC standard errors.

The estimates have economic interpretations:

Spatial diffusion $\hat{\nu}_s = 98$ square miles per quarter implies annual mobility scale of approximately 20 miles, consistent with commuting distances.

Decay rate $\hat{\kappa} = 0.28$ implies 2.5-quarter half-life, consistent with gradual labor market adjustment.

Mutual information $\hat{I}(\mathbf{x}; \alpha) = 0.38$ quantifies spatial clustering of supply chains.

The Hansen J -test passes ($p = 0.47$), supporting correct specification.

4.4 Comparison with Conventional Methods

Table 6 compares methods.

Table 6: Comparison of Estimation Methods

Method	Direct	Spatial	Network	Mixed	Total
TWFE	0.031	—	—	—	0.031
Continuous GPS	0.042	—	—	—	0.042
No-spillover PDE	0.044	—	—	—	0.044
Full PDE	0.041	0.041	0.028	0.043	0.153

Notes: Effects at state border. Total for Full PDE is $3.7\times$ direct.

Conventional methods estimate direct effects of \$0.031–0.044. The Full PDE estimates total effects of \$0.153 at the border—3.7 times larger. Conventional methods capture only 27% of total policy impact.

4.5 Decomposition

At the border, direct effects account for 27% of total; spatial spillovers 27%, network spillovers 16%, and mixed effects 30%. The mixed effect—synergistic amplification when both channels reinforce each other—accounts for nearly one-third of total impact.

5 Conclusion

This paper develops a continuous functional framework for treatment effects that propagate through geographic space and economic networks. The theoretical contribution derives a master equation from three independent foundations—heterogeneous agent aggregation, market equilibrium, and cost minimization—with key results including the Feynman-Kac representation and the mutual information characterization of spatial-network interaction.

The methodological contribution establishes that the framework nests the no-spillover case as a testable restriction, creating a one-sided risk profile: correct inference regardless of whether spillovers exist. Monte Carlo evidence with both binary treatment timing and continuous treatment intensity confirms that conventional methods exhibit substantial bias (25–38%) when spillovers are present, while our framework maintains correct inference across all configurations.

The empirical contribution, applying the framework to minimum wage policy, finds total effects four times larger than direct effects, demonstrating the quantitative importance of spillover channels. Structural parameter estimates have economic interpretations consistent with labor market mobility and supply chain adjustment.

5.1 Limitations

The framework assumes continuous treatment functionals, which may not apply to perfectly discrete interventions. The identification strategy requires geographic and network variation; uniformly implemented policies remain unidentified. The entropy-based diagnostics require additional validation across settings.

5.2 Extensions

Several directions appear promising:

Heterogeneous agents: Full development of type-specific parameters $(\nu_s(\theta), \nu_n(\theta), \kappa(\theta))$ would enable distributional analysis.

Optimal policy: Characterizing the optimal source $S^*(\mathbf{x}, t, \alpha)$ would provide normative guidance.

Alternative applications: The framework applies to financial contagion, technology diffusion, disease transmission, and trade policy—settings where spatial-network propagation matters.

References

- Acemoglu, D., V. M. Carvalho, A. Ozdaglar, and A. Tahbaz-Salehi (2012). The network origins of aggregate fluctuations. *Econometrica* 80(5), 1977–2016.
- Acemoglu, D., A. Ozdaglar, and A. Tahbaz-Salehi (2016). Networks, shocks, and systemic risk. In Y. Bramoullé, A. Galeotti, and B. Rogers (Eds.), *The Oxford Handbook of the Economics of Networks*, pp. 569–607. Oxford University Press.
- Aiyagari, S. R. (1994). Uninsured idiosyncratic risk and aggregate saving. *Quarterly Journal of Economics* 109(3), 659–684.
- Anderson, P. W. (1972). More is different. *Science* 177(4047), 393–396.
- Anselin, L. (1988). *Spatial Econometrics: Methods and Models*. Kluwer Academic Publishers.
- Anselin, L. (2010). Thirty years of spatial econometrics. *Papers in Regional Science* 89(1), 3–25.
- Athey, S., D. Eckles, and G. W. Imbens (2018). Exact p-values for network interference. *Journal of the American Statistical Association* 113(521), 230–240.
- Autor, D. H., A. Manning, and C. L. Smith (2016). The contribution of the minimum wage to US wage inequality over three decades: A reassessment. *American Economic Journal: Applied Economics* 8(1), 58–99.
- Barrot, J.-N. and J. Sauvagnat (2016). Input specificity and the propagation of idiosyncratic shocks in production networks. *Quarterly Journal of Economics* 131(3), 1543–1592.
- Beirlant, J., E. J. Dudewicz, L. Györfi, and E. C. van der Meulen (1997). Nonparametric entropy estimation: An overview. *International Journal of Mathematical and Statistical Sciences* 6(1), 17–39.

- Benamou, J.-D. and Y. Brenier (2000). A computational fluid mechanics solution to the Monge-Kantorovich mass transfer problem. *Numerische Mathematik* 84(3), 375–393.
- Bertrand, M., E. Duflo, and S. Mullainathan (2004). How much should we trust differences-in-differences estimates? *Quarterly Journal of Economics* 119(1), 249–275.
- Bramoullé, Y., H. Djebbari, and B. Fortin (2009). Identification of peer effects through social networks. *Journal of Econometrics* 150(1), 41–55.
- Callaway, B. and P. H. C. Sant’Anna (2021). Difference-in-differences with multiple time periods. *Journal of Econometrics* 225(2), 200–230.
- Caliendo, L., M. Dvorkin, and F. Parro (2019). Trade and labor market dynamics: General equilibrium analysis of the China trade shock. *Econometrica* 87(3), 741–835.
- Calonico, S., M. D. Cattaneo, and R. Titiunik (2014). Robust nonparametric confidence intervals for regression-discontinuity designs. *Econometrica* 82(6), 2295–2326.
- Card, D. (2001). Immigrant inflows, native outflows, and the local labor market impacts of higher immigration. *Journal of Labor Economics* 19(1), 22–64.
- Card, D. and A. B. Krueger (1994). Minimum wages and employment: A case study of the fast-food industry in New Jersey and Pennsylvania. *American Economic Review* 84(4), 772–793.
- Cengiz, D., A. Dube, A. Lindner, and B. Zipperer (2019). The effect of minimum wages on low-wage jobs. *Quarterly Journal of Economics* 134(3), 1405–1454.
- Cercignani, C. (1988). *The Boltzmann Equation and Its Applications*. Springer-Verlag.

- Conley, T. G. (1999). GMM estimation with cross sectional dependence. *Journal of Econometrics* 92(1), 1–45.
- Conley, T. G. and C. R. Taber (2011). Inference with “difference in differences” with a small number of policy changes. *Review of Economics and Statistics* 93(1), 113–125.
- Cover, T. M. and J. A. Thomas (2006). *Elements of Information Theory* (2nd ed.). Wiley-Interscience.
- de Chaisemartin, C. and X. D’Haultfoeulle (2020). Two-way fixed effects estimators with heterogeneous treatment effects. *American Economic Review* 110(9), 2964–2996.
- Dube, A. (2019). Impacts of minimum wages: Review of the international evidence. Report commissioned by HM Treasury, UK Government.
- Dube, A., T. W. Lester, and M. Reich (2010). Minimum wage effects across state borders: Estimates using contiguous counties. *Review of Economics and Statistics* 92(4), 945–964.
- Elliott, M., B. Golub, and M. O. Jackson (2014). Financial networks and contagion. *American Economic Review* 104(10), 3115–3153.
- Ellison, G. and E. L. Glaeser (1997). Geographic concentration in U.S. manufacturing industries: A dartboard approach. *Journal of Political Economy* 105(5), 889–927.
- Evans, L. C. (2010). *Partial Differential Equations* (2nd ed.). American Mathematical Society.
- Gelfand, I. M. and S. V. Fomin (1963). *Calculus of Variations*. Prentice-Hall. Reprinted by Dover, 2000.

- Goodman-Bacon, A. (2021). Difference-in-differences with variation in treatment timing. *Journal of Econometrics* 225(2), 254–277.
- Hansen, L. P. (1982). Large sample properties of generalized method of moments estimators. *Econometrica* 50(4), 1029–1054.
- Heckman, J. J. (1979). Sample selection bias as a specification error. *Econometrica* 47(1), 153–161.
- Heckman, J. J. (2001). Micro data, heterogeneity, and the evaluation of public policy: Nobel lecture. *Journal of Political Economy* 109(4), 673–748.
- Heckman, J. J. and B. Singer (1984). A method for minimizing the impact of distributional assumptions in econometric models for duration data. *Econometrica* 52(2), 271–320.
- Hirano, K. and G. W. Imbens (2004). The propensity score with continuous treatments. In A. Gelman and X.-L. Meng (Eds.), *Applied Bayesian Modeling and Causal Inference from Incomplete-Data Perspectives*, pp. 73–84. Wiley.
- Hudgens, M. G. and M. E. Halloran (2008). Toward causal inference with interference. *Journal of the American Statistical Association* 103(482), 832–842.
- Huggett, M. (1993). The risk-free rate in heterogeneous-agent incomplete-insurance economies. *Journal of Economic Dynamics and Control* 17(5–6), 953–969.
- Imbens, G. W. (2004). Nonparametric estimation of average treatment effects under exogeneity: A review. *Review of Economics and Statistics* 86(1), 4–29.
- Imbens, G. W. and J. D. Angrist (1994). Identification and estimation of local average treatment effects. *Econometrica* 62(2), 467–475.
- Imbens, G. W. and J. M. Wooldridge (2009). Recent developments in the econometrics of program evaluation. *Journal of Economic Literature* 47(1), 5–86.

- Jackson, M. O. (2008). *Social and Economic Networks*. Princeton University Press.
- Jordan, R., D. Kinderlehrer, and F. Otto (1998). The variational formulation of the Fokker-Planck equation. *SIAM Journal on Mathematical Analysis* 29(1), 1–17.
- Kaminsky, G. L. and C. M. Reinhart (1999). The twin crises: The causes of banking and balance-of-payments problems. *American Economic Review* 89(3), 473–500.
- Kaplan, G., B. Moll, and G. L. Violante (2018). Monetary policy according to HANK. *American Economic Review* 108(3), 697–743.
- Keele, L. J. and R. Titiunik (2015). Geographic boundaries as regression discontinuities. *Political Analysis* 23(1), 127–155.
- Kelejian, H. H. and I. R. Prucha (1998). A generalized spatial two-stage least squares procedure for estimating a spatial autoregressive model with autoregressive disturbances. *Journal of Real Estate Finance and Economics* 17(1), 99–121.
- Kennedy, E. H., Z. Ma, M. D. McHugh, and D. S. Small (2017). Non-parametric methods for doubly robust estimation of continuous treatment effects. *Journal of the Royal Statistical Society: Series B* 79(4), 1229–1245.
- Krusell, P. and A. A. Smith, Jr. (1998). Income and wealth heterogeneity in the macroeconomy. *Journal of Political Economy* 106(5), 867–896.
- Kubo, R. (1966). The fluctuation-dissipation theorem. *Reports on Progress in Physics* 29(1), 255–284.
- Lee, D. S. and T. Lemieux (2010). Regression discontinuity designs in economics. *Journal of Economic Literature* 48(2), 281–355.
- Lee, D. and E. Saez (2012). Optimal minimum wage policy in competitive labor markets. *Journal of Public Economics* 96(9–10), 739–749.

- LeRoy, S. F. (1973). Risk aversion and the martingale property of stock prices. *International Economic Review* 14(2), 436–446.
- LeSage, J. P. and R. K. Pace (2009). *Introduction to Spatial Econometrics*. CRC Press.
- Manning, A. (2003). *Monopsony in Motion: Imperfect Competition in Labor Markets*. Princeton University Press.
- Manski, C. F. (1993). Identification of endogenous social effects: The reflection problem. *Review of Economic Studies* 60(3), 531–542.
- Melitz, M. J. (2003). The impact of trade on intra-industry reallocations and aggregate industry productivity. *Econometrica* 71(6), 1695–1725.
- Moretti, E. (2011). Local labor markets. In O. Ashenfelter and D. Card (Eds.), *Handbook of Labor Economics*, Volume 4B, pp. 1237–1313. Elsevier.
- Müller, U. K. and M. W. Watson (2022). Spatial correlation robust inference. *Econometrica* 90(6), 2901–2935.
- Müller, U. K. and M. W. Watson (2024). Spatial unit roots and spurious regression. *Econometrica* 92(5), 1661–1695.
- Neumark, D. and W. L. Wascher (2008). *Minimum Wages*. MIT Press.
- Newey, W. K. and K. D. West (1987). A simple, positive semi-definite, heteroskedasticity and autocorrelation consistent covariance matrix. *Econometrica* 55(3), 703–708.
- Oates, W. E. (1972). *Fiscal Federalism*. Harcourt Brace Jovanovich.
- Øksendal, B. (2003). *Stochastic Differential Equations: An Introduction with Applications* (6th ed.). Springer.

- Roback, J. (1982). Wages, rents, and the quality of life. *Journal of Political Economy* 90(6), 1257–1278.
- Rosen, S. (1979). Wage-based indexes of urban quality of life. In P. Mieszkowski and M. Straszheim (Eds.), *Current Issues in Urban Economics*, pp. 74–104. Johns Hopkins University Press.
- Rosenbaum, P. R. and D. B. Rubin (1983). The central role of the propensity score in observational studies for causal effects. *Biometrika* 70(1), 41–55.
- Rubin, D. B. (1974). Estimating causal effects of treatments in randomized and nonrandomized studies. *Journal of Educational Psychology* 66(5), 688–701.
- Samuelson, P. A. (1965). Proof that properly anticipated prices fluctuate randomly. *Industrial Management Review* 6(2), 41–49.
- Sun, L. and S. Abraham (2021). Estimating dynamic treatment effects in event studies with heterogeneous treatment effects. *Journal of Econometrics* 225(2), 175–199.
- Wooldridge, J. M. (2010). *Econometric Analysis of Cross Section and Panel Data* (2nd ed.). MIT Press.